

Distance Cartogram Construction for Visualizing Motion-characteristic Distribution of Bon Odori Dances in Akita Prefecture

Takeshi Miura (Graduate School of Engineering Science, Akita University)
 Takeshi Shibata (Graduate School of Science and Engineering, Ibaraki University)
 Madoka Uemura (Faculty of Education and Human Studies, Akita University)
 Katsubumi Tajima (Graduate School of Engineering Science, Akita University)
 Hideo Tamamoto (Tohoku University of Community Service and Science)

In Akita Prefecture, Japan, many Bon Odori dances (Bon Odori: one of the Japanese folk dance categories) have been passed down in respective regional communities. To visualize relationship between the regional motion-characteristic variation of Bon Odori dances and the geographic elements of corresponding regions in Akita Prefecture, a technique of map deformation was introduced in a previous study. As a result, a deformed map having the style of distance cartogram was constructed. However, the geometrical characteristics of the original geographic elements, e.g., the smoothness of the original shapes, were not necessarily maintained. In this study, we apply a technique of moving least squares transformation to the Bon Odori distance cartogram construction. This technique guarantees globally smooth deformation. We also propose a new performance index quantitatively evaluating the degree of deformation of the obtained cartogram. This is introduced to avoid excessive deformation that deteriorates the readability of the cartogram. Experimental results demonstrate the effectiveness of the proposed approach to a certain extent.

1. Introduction

In Akita Prefecture, Japan, many *Bon Odori* dances*¹ have been passed down in respective regional communities, and each dance has been strongly affected by the geographic and cultural conditions of each region. In Ref. [1], a technique of map deformation was introduced to visualize the relationship between the regional motion-characteristic variation of *Bon Odori* dances and the geographic elements of corresponding regions in Akita Prefecture. As a result, a deformed map having the style of distance cartogram [2] was constructed.

In a distance cartogram, the distance of each of the preselected point pairs in the geographic map is changed in step with a specified value. The construction process of a distance cartogram generally consists of two steps [3]. The locations of the points included in the preselected pairs are fixed in the first step, whereas the locations of other points are fixed in the second step. Several effective approaches have been proposed for the first step [2],[4]. As for the second step, the combination of triangulation and barycentric interpolation [4] has been often used as a classical technique (In fact, this classical technique was used in Ref. [1] for constructing the *Bon Odori* distance cartogram.).

On the other hand, recently, the application of the moving least squares (MLS) transformation technique to the second step has been proposed [3],[5]. This technique guarantees globally smooth deformation [6],

which is not satisfied by the combination of triangulation and barycentric interpolation. In this study, we apply the MLS technique to the second step of the *Bon Odori* cartogram construction. We also introduce a new performance index quantitatively evaluating the degree of deformation of the obtained cartogram. This is introduced to avoid excessive deformation that deteriorates the readability of the cartogram.

2. *Bon Odori* Dances of Akita Prefecture

2.1 Distribution of *Bon Odori* Dances in Akita Prefecture

Table 1 shows the *Bon Odori* dances of Akita Prefecture investigated in this study. As shown in the table, the dances investigated are classified into three groups*² and have been passed down in ten settlements. To construct the *Bon Odori* cartogram in which the configuration of the settlements is changed based on the dance features of the *Bon Odori* dances, the motion characteristics of the above dances are quantitatively extracted by numerically analyzing motion capture (Mocap) data. The set of the Mocap data used in the numerical analysis is also shown in Table 1 (the dataset identical to that in Ref. [1] is used).

Figure 1 shows the geographic map of Akita Prefecture. The distribution of the ten settlements and the

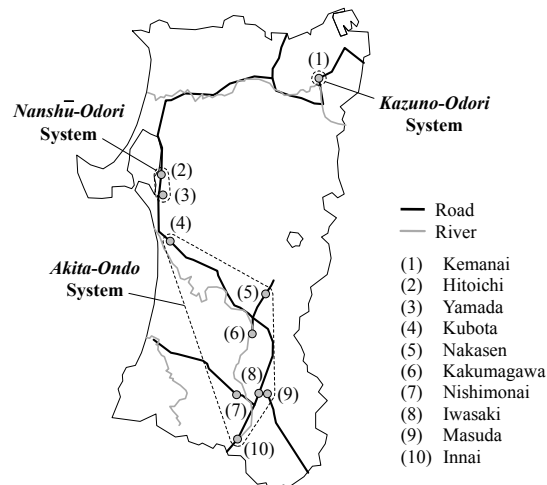
*¹ *Bon Odori* is a type of Japanese folk dance performed during the annual Buddhist festival called *O-Bon* (or simply *Bon*).

*² The *Bon Odori* dances of Akita Prefecture have been classified into four groups: *Kazuno-Odori*, *Nanshū-Odori*, *Akita-Ondo* and *Yuri-Bon-Odori* Systems [7]. However, most of the dances belonging to the *Yuri-Bon-Odori* System have been lost until now [8]. Therefore, only the dances belonging to the remaining three groups are investigated in this study.

Table 1 *Bon Odori* dances of Akita Prefecture

| Group | Settlement | Dance | Mocap data (No., time) |
|--------------------------|------------|---------------------------|---------------------------|
| Kazuno-Odori System | Kemanai | <i>Dainosaka</i> | 3*, 10.8 s |
| | | <i>Jinku</i> | 3*, 9.9 s |
| Nanshū-Odori System | Hitoichi | <i>Dendenzuku</i> | 3*, 6.6 s |
| | | <i>Kitasaka</i> | 6*, 5.5 s |
| | | <i>Sankatsu</i> | 4*, 11.6 s |
| | | | |
| | Yamada | <i>Kitasaka</i> | 5#, 5.5 s |
| | | <i>Dagasuko</i> | 4#, 6.9 s |
| | | <i>Sankatsu</i> | 5#, 11.8 s |
| | | | |
| Akita-Ondo System | Kubota | <i>Akita Ondo</i> | 1*, 67.8 s |
| | Nakasen | <i>Donpan Odori</i> | 1*, 33.8 s |
| | | <i>Emazō Jinku</i> | 1*, 32.7 s |
| | Kakumagawa | (no name) | 1*, 59.3 s |
| | Nishimonai | <i>Ondo</i> | 3*, 44.5 s |
| | | <i>Ganke</i> | 3*, 41.1 s |
| | Iwasaki | <i>Otoko Odori</i> | 1*, 72.6 s |
| | | <i>Onna Odori</i> | 1*, 73.8 s |
| | Masuda | (no name) | 2*, 69.2 s |
| | Innai | <i>Innai Ginzan Odori</i> | 4*, 29.3 s |
| <i>Innai Ginzan Ondo</i> | | 2*, 39.3 s | |

Mocap data: provided by Warabi-za Co., Ltd. (*) and the Center of Community (COC) Project of Akita University (#), time: mean time of all the Mocap data streams in a single dance.

**Fig. 1** Geographic map of Akita Prefecture

geographic elements including roads, rivers and lakes is indicated in the map. It is seen that the three *Bon Odori* groups are geographically separated. In the distance cartogram construction process, the ten settlements are used as points constituting a set of the point pairs whose configuration in the cartogram is fixed in the first step of the process. The next section describes how to calculate newly specified distance values given to the pairs to fix their configuration in the first step.

2.2 Calculation of Between-settlement Distances Representing the Motion-characteristic Similarity of *Bon Odori* Dances

As mentioned in Section 1, the configuration of the ten settlements in the cartogram is fixed by changing the between-settlement distance of each point pair in step with a newly specified distance. In the present *Bon-Odori*-cartogram construction case, a quantity representing the motion-characteristic similarity of *Bon Odori* dances is used to specify each new distance value. Specifically, the method proposed in Ref. [1] is used to obtain the new values as follows.

In the method, the motion characteristics of each Mocap data stream is first extracted by phase plane analysis [9]. This approach provides motion-characteristic quantities of each Mocap data stream in the form of a simple low-dimensional feature vector having only six components (average motion amount and motion complexity, each of which is quantified for each of the three axes of movement, i.e., the frontal, vertical and sagittal axes [10]). The distance of a pair of Mocap data streams is obtained by calculating the Euclidean distance between their feature vectors.

Then, the distance of each dance pair is calculated.

In general, each dance investigated in this study includes multiple Mocap data streams as shown in Table 1. In other words, each dance consists of a set of Mocap data streams. Therefore, we use the Earth Mover's Distance (EMD) known as a representative between-set distance [11] as the between-dance distance. Finally, the distance of each settlement pair is calculated. As with the case of the between-dance distance, each settlement generally consists of a set of dances. Therefore, we again use the EMD as the between-settlement distance.

3. Cartogram Construction

3.1 Overview of Moving Least Squares Transformation in Cartogram Construction

In the first step of the *Bon Odori* cartogram construction, we fix the configuration of the settlements using the above between-settlement distance dataset representing the motion-characteristic similarity of the *Bon Odori* dances in each settlement pair. We apply the distance cartogram construction algorithm of Ref. [2] to the dataset. In the second step, on the other hand, the configuration of geographic elements including roads, rivers, lakes and the outline of Akita Prefecture is determined as follows.

We assume that the position of the i th settlement in the geographic map is given as $\mathbf{p}_G(i) = [x_G(i) \ y_G(i)]$, and was already converted in the first step into the new position $\mathbf{p}_C(i) = [x_C(i) \ y_C(i)]$ in the cartogram. In the second step, we select a point belonging to any of the geographic elements in the geographic map (position in the geographic map: $\mathbf{p}_{G0} = [x_{G0} \ y_{G0}]$). The position of this point in the cartogram, $\mathbf{p}_{C0} = [x_{C0} \ y_{C0}]$, is fixed by MLS as follows [6]:

$$\mathbf{p}_{C0} = (\mathbf{p}_{G0} - \bar{\mathbf{p}}_G)\mathbf{M} + \bar{\mathbf{p}}_C \quad (1)$$

$$\bar{\mathbf{p}}_G = \frac{\sum_{i=1}^N w(i) \mathbf{p}_G(i)}{\sum_{i=1}^N w(i)}, \quad \bar{\mathbf{p}}_C = \frac{\sum_{i=1}^N w(i) \mathbf{p}_C(i)}{\sum_{i=1}^N w(i)}$$

where \mathbf{M} is the linear transformation matrix, N is the number of settlements and $w(i)$ is the weight function given to the i th settlement. \mathbf{M} can be obtained by any of the following three approaches: affine transformation, similarity transformation and rigid transformation [6] (Details will be described in Sections 3.2, 3.3 and 3.4.). As for $w(i)$, we use the following procedure [5]:

- (1) Let $w(i) = 1/|\mathbf{p}_G(i) - \mathbf{p}_{G0}|^4$ for $1 \leq i \leq N$.
- (2) Obtain \mathbf{p}_{C0} by Eq. (1).
- (3) Let $w(i) = \{w(i)/|\mathbf{p}_C(i) - \mathbf{p}_{C0}|^4\}^{1/2}$ for $1 \leq i \leq N$.
- (4) Obtain \mathbf{p}_{C0} by Eq. (1) (using the modified $w(i)$).

The above procedure makes it possible to reflect the information on not only the geographic map but also the cartogram, thereby improving robustness against the violation of homeomorphism occurring frequently in a highly deformed cartogram [5].

3.2 Affine Transformation

In the affine transformation approach, the linear transformation matrix \mathbf{M} is obtained by minimizing the following objective function f [6]:

$$f = \sum_{i=1}^N w(i) |\hat{\mathbf{p}}_G(i) \mathbf{M} - \hat{\mathbf{p}}_C(i)|^2 \quad (2)$$

$$\hat{\mathbf{p}}_G(i) = \mathbf{p}_G(i) - \bar{\mathbf{p}}_G, \quad \hat{\mathbf{p}}_C(i) = \mathbf{p}_C(i) - \bar{\mathbf{p}}_C$$

The above objective function is the weighted sum of squared estimate of errors. By solving the above optimization problem, we can fix \mathbf{M} as follows:

$$\mathbf{M} = \left\{ \sum_{i=1}^N \hat{\mathbf{p}}_G(i)^T w(i) \hat{\mathbf{p}}_G(i) \right\}^{-1} \sum_{j=1}^N w(j) \hat{\mathbf{p}}_G(j)^T \hat{\mathbf{p}}_C(j) \quad (3)$$

The above solution is obtained by using the classical normal least squares technique [12].

3.3 Similarity Transformation

In the affine transformation approach, the moving least squares optimization problem is solved without any constraint. This can cause undesired deformation such as excessive non-uniform scaling [6]. To improve the property of preventing undesired deformation, the region of transformation is restricted in the similarity transformation approach. Specifically, the allowable region of transformation is limited to a special subset of affine transformations that only include translation, rotation and uniform scaling [6]. This means that \mathbf{M} must satisfy the condition $\mathbf{M}^T \mathbf{M} = \lambda^2 \mathbf{I}$ for some scalar λ . As a result, \mathbf{M} is determined as follows:

$$\mathbf{M} = \frac{1}{\mu_s} \sum_{i=1}^N w(i) \begin{bmatrix} \hat{\mathbf{p}}_G(i) \\ -\hat{\mathbf{p}}_G(i)^\perp \end{bmatrix} [\hat{\mathbf{p}}_C(i)^T \quad -\hat{\mathbf{p}}_C(i)^{\perp T}] \quad (4)$$

$$\mu_s = \sum_{i=1}^N w(i) \hat{\mathbf{p}}_G(i) \hat{\mathbf{p}}_G(i)^T$$

where $[x \ y]^\perp = [-y \ x]$. The above \mathbf{M} maintains similarity between a figure in the geographic map and the corresponding figure in the cartogram.

3.4 Rigid Transformation

In the rigid transformation approach, the moving least squares optimization problem is solved under a more strict constraint than that of similarity transformation. Specifically, the allowable region of transformation is more narrowly limited to that which only includes translation and rotation (This transformation corresponds to the motion of a rigid body.) [6]. As a result, \mathbf{M} is determined as follows:

$$\mathbf{M} = \frac{\rho_r}{\mu_r} \sum_{i=1}^N w(i) \begin{bmatrix} \hat{\mathbf{p}}_G(i) \\ -\hat{\mathbf{p}}_G(i)^\perp \end{bmatrix} [\hat{\mathbf{p}}_C(i)^T \quad -\hat{\mathbf{p}}_C(i)^{\perp T}] \quad (5)$$

$$\rho_r = \frac{\sum_{i=1}^N w(i) |\hat{\mathbf{p}}_C(i)|}{\sum_{i=1}^N w(i) |\hat{\mathbf{p}}_G(i)|}$$

$$\mu_r = \sqrt{\left\{ \sum_{i=1}^N w(i) \hat{\mathbf{p}}_C(i) \hat{\mathbf{p}}_G(i)^T \right\}^2 + \left\{ \sum_{i=1}^N w(i) \hat{\mathbf{p}}_C(i) \hat{\mathbf{p}}_G(i)^{\perp T} \right\}^2}$$

The matrix \mathbf{M}/ρ_r maintains congruence between a figure in the geographic map and the corresponding figure in the cartogram, i.e. satisfies the condition $(\mathbf{M}/\rho_r)^T (\mathbf{M}/\rho_r) = \mathbf{I}$. The coefficient ρ_r is introduced to perform the scale conversion from the geographic map into the cartogram.

3.5 Cartogram Construction for a Simple Artificial Mapping Model

Figure 2. shows examples of cartogram construction for a simple artificial mapping model. In the model, the geographic map consists of six points and ten regular-interval parallel lines. The configuration of the points in the cartogram is fixed in the first step of cartogram construction in advance (The highest point in the geographic map is moved downward.). Then, the configuration of the ten lines in the cartogram is fixed in the second step based on the locations of the six points.

In the case that the combination of the Delaunay triangulation and barycentric interpolation [4] is used in the second step, many non-differentiable points and the violation of homeomorphism are seen. On the other hand, in the cases that the MLS approaches are used, all the ten lines are smoothly deformed without the appearance of non-differentiable point that does not exist in the original lines of the geographic map, although the violation of homeomorphism is seen only in the case of rigid transformation. The above examples suggest that applying the MLS technique to the second step of distance cartogram construction is

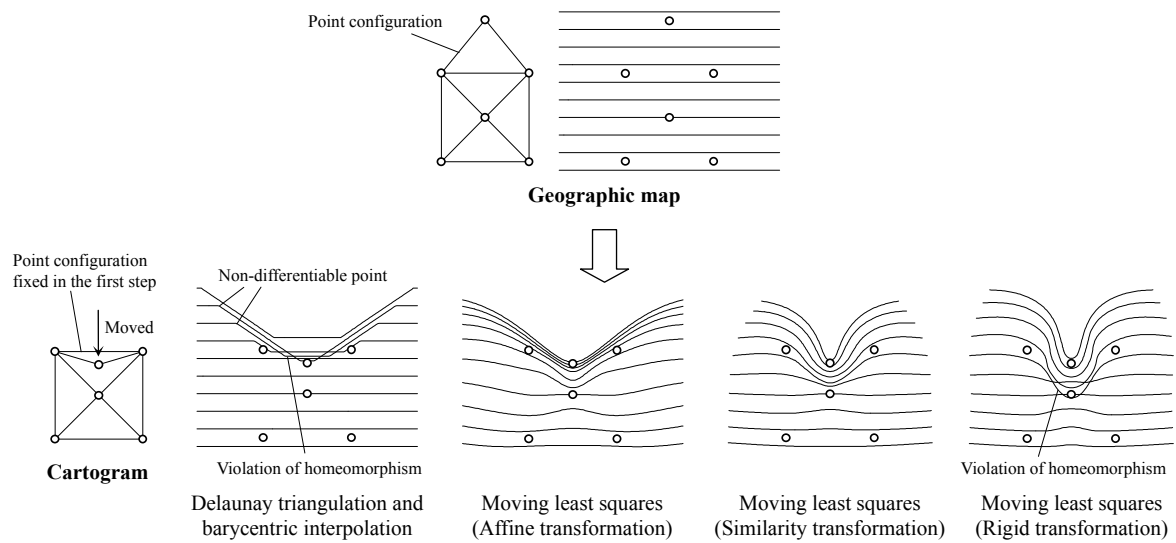


Fig. 2 Cartogram construction for an artificial mapping model.

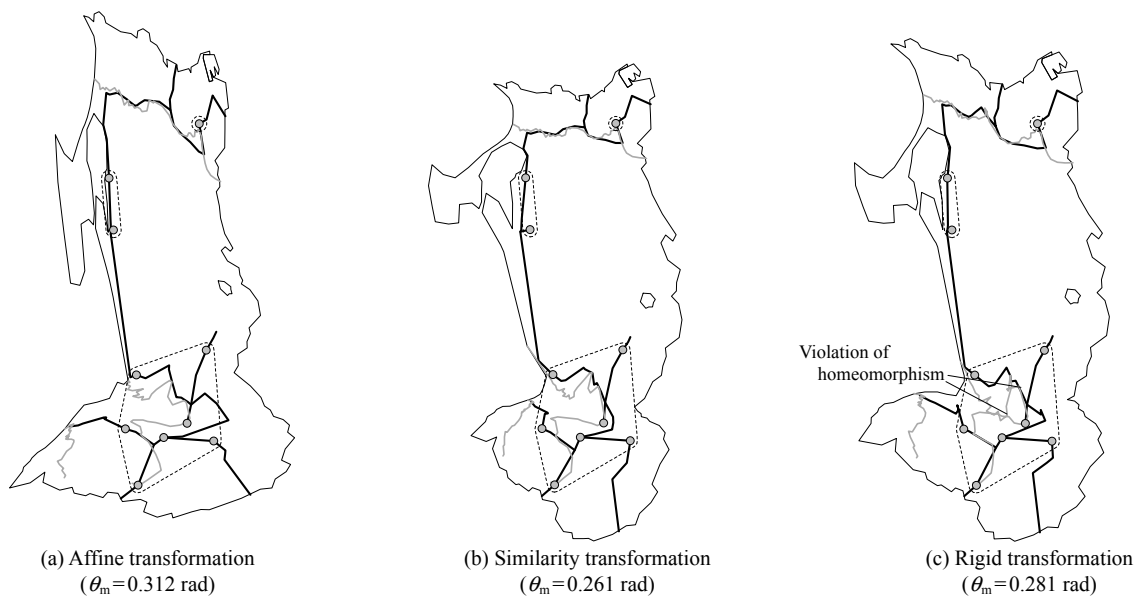


Fig. 3 Distance cartograms obtained by moving least squares transformation. (Settlement configuration (obtained in the first step): identical in all cartograms)

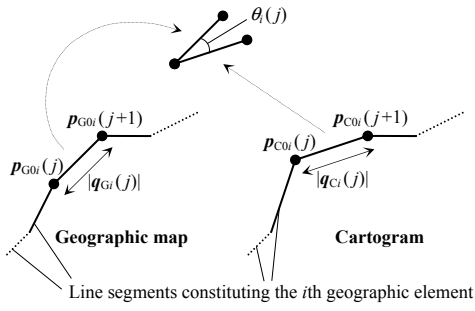
effective to improve the property of maintaining the global smoothness.

4. Results and Discussion

Figure 3 shows the *Bon Odori* distance cartograms of Akita Prefecture obtained by analyzing the Mocap data of Table 1. As already mentioned in Section 3.1, the configuration of the ten settlements is fixed in the first step in advance (The distance cartogram construction algorithm of Ref. [2] is applied to the between-settlement distance dataset.). As for the second

step, the three MLS approaches, i.e., the affine transformation, similarity transformation and rigid transformation approaches, are applied.

To maintain the readability of the cartogram, excessive deformation should be avoided. Here, we quantitatively evaluate the degree of the deformation of each cartogram. Figure 4 shows the concept of the quantitative evaluation of map deformation. As shown in the figure, we use the weighted mean of angles each of which is formed by a line segment constituting any of the geographic elements in the geographic map and the corresponding line segment



Weighted mean of $\theta_i(j)$'s (weight: geometric mean of $|q_{Gi}(j)|$ and $|q_{Ci}(j)|$):

$$\theta_m = \frac{\sum_{i=1}^{N_{GE}} \sum_{j=1}^{N_{GE_i}-1} \{|q_{Gi}(j)| |q_{Ci}(j)|\}^{1/2} \theta_i(j)}{\sum_{i=1}^{N_{GE}} \sum_{j=1}^{N_{GE_i}-1} \{|q_{Gi}(j)| |q_{Ci}(j)|\}^{1/2}}$$

Fig. 4 Quantitative evaluation of map deformation.

in the cartogram (weight: geometric mean of the lengths of these two line segments):

$$\theta_m = \frac{\sum_{i=1}^{N_{GE}} \sum_{j=1}^{N_{GE_i}-1} \{|q_{Gi}(j)| |q_{Ci}(j)|\}^{1/2} \theta_i(j)}{\sum_{i=1}^{N_{GE}} \sum_{j=1}^{N_{GE_i}-1} \{|q_{Gi}(j)| |q_{Ci}(j)|\}^{1/2}} \quad (6)$$

$$q_{Gi}(j) = p_{G0i}(j+1) - p_{G0i}(j),$$

$$q_{Ci}(j) = p_{C0i}(j+1) - p_{C0i}(j),$$

$$\theta_i(j) = \text{atan2}(\alpha_i(j), \sqrt{1 - \alpha_i(j)^2}),$$

$$\alpha_i(j) = q_{Gi}(j) \cdot q_{Ci}(j) / \{|q_{Gi}(j)| |q_{Ci}(j)|\},$$

$$p_{G0i}(j) = [x_{G0i}(j) \quad y_{G0i}(j)],$$

$$p_{C0i}(j) = [x_{C0i}(j) \quad y_{C0i}(j)]$$

where N_{GE} is the number of geographic elements, N_{GE_i} is the number of points constituting the i th geographic element, $p_{G0i}(j)$ and $p_{C0i}(j)$ are the position of the j th point constituting the i th geographic element in the geographic map and that in the cartogram, respectively.

In Fig. 3, the cartogram (a) obtained by affine transformation gives the largest θ_m . In fact, a remarkable deformation of (a) can be visually grasped, and θ_m appropriately quantifies this tendency. The cartogram (b) obtained by similarity transformation, which gives the smallest θ_m , shows a moderate deformation causing no problem in practical use. On the other hand, the violation of homeomorphism is seen in (c) obtained by rigid transformation, even though the θ_m value of (c) is smaller than that of (a). This suggests that not only quantitative evaluation but also qualitative evaluation may be needed. Hereinafter, we adopt the cartogram (b) as the definitive version obtained by the proposed approach.

Figure 5 shows comparison between the original geographic map of Akita Prefecture and the *Bon Odori* distance cartogram obtained by similarity

transformation. As already pointed out in Ref. [1], the *Bon Odori* cartogram of Akita Prefecture shows two distinctive features. One is the shortening of the distance between the *Kazuno-Odori* and *Nanshū-Odori* Systems, and the other is a remarkable southward movement of the Kubota settlement. One can notice that both are caused by the shortening of the road-river dual-path route*³ (former: *Ushū Kaidō* and *Jūnisho Kaidō* Roads and Yoneshiro River, latter: *Ushū Kaidō* Road and Omono River). This suggests the influence of traffic networks on the transmission of the motion characteristics of *Bon Odori* dances, and the cartogram obtained by the proposed approach clearly visualizes the above tendency.

The proposed method is applicable to an arbitrary dance category as long as its regional distribution can be represented as a hierarchical model having the group-settlement-dance hierarchical structure shown in Table 1. This suggests that the influence of geographic factors on the regional distribution of folk dances other than the *Bon Odori* dances of Akita Prefecture can be also schematically represented, and the obtained cartogram would help attract renewed attention to the study of the folk dances with a visual impact.

5. Conclusion

In this study, we applied the MLS technique to the *Bon Odori* distance cartogram construction, and quantitatively evaluated the obtained cartograms. The effectiveness of the proposed approach was demonstrated to a certain extent. To confirm the application range will be the subject of future work.

Acknowledgments This study was supported by JSPS Grants-in-Aid for Scientific Research (KAKENHI) Grant Number JP18K11981. The motion capture data of the *Bon Odori* dances passed down in the Yamada districts were provided by Akita University's Center of Community Project "Regional Development Aimed at Promoting an Independent Aging Society in Which All Individuals Have Value." The other motion capture data were provided by Warabi-za, Co., Ltd.

References

- [1] Miura, T., Shibata, T., Uemura, M., Tajima, K. and Tamamoto, H.: Visualization of Motion and Geographic Characteristics of Bon Odori Dances in Akita Prefecture, *IPSSJ Symposium Series*, Vol.2018, No.1, pp.359-364 (2018).
- [2] Shimizu, E. and Inoue, R.: A New Algorithm for Distance Cartogram Construction, *International Journal of Geographical Information Science*,

*³ In the early-modern times (i.e., the period *Bon Odori* dances spread around the country), most of the rivers in Akita Prefecture were used as water routes.

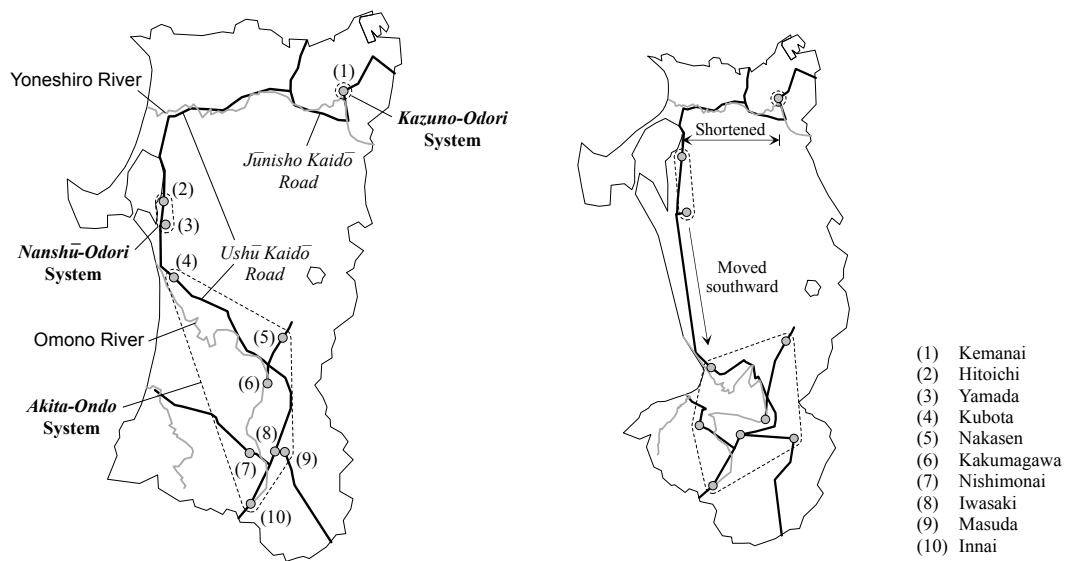


Fig. 5 Comparison between the original geographic map of Akita Prefecture (left) and the *Bon Odori* distance cartogram (right, obtained by similarity transformation).

- Vol.23, No.11, pp.1453-1470 (2009).
- [3] Ullah, R. and Kraak, M.-J.: An Alternative Method to Constructing Time Cartograms for the Visual Representation of Scheduled Movement Data, *Journal of Maps*, Vol.11, No.4, pp. 674-687 (2015).
- [4] Bies, S. and van Kreveld, M.: Time-Space Maps from Triangulations, Didimo, W. and Patrignani, M. (Eds.): *GD 2012, LNCS 7704*, pp.511-516 (2013).
- [5] Miura, T. and Tajima, K.: Improvement of Moving Least Squares Transformation in Distance Cartogram Construction, *IEEJ Trans. on Electrical and Electronic Engineering*, Vol.14, No.12 (2019) (in press).
- [6] Schaefer, S., T. McPhail, T. and Warren, J.: Image Deformation Using Moving Least Squares, *ACM Trans. on Graphics*, Vol.25, No.3, pp.533-540 (2006).
- [7] Japan Broadcasting Corporation (ed.): *Tōhoku Min'yōshū Akita Ken (A Collection of Folk Songs of Tōhoku Region: Akita Prefecture)*, Japan Broadcast Publishing Association (1957) (in Japanese).
- [8] Miura, T., Kaiga, T., Shibata, T., Katsura, H., Tajima, K. and Tamamoto, H.: Utilization of Motion Capture Data for Research on Folk Performing Arts of Akita Prefecture, *IPSJ SIG Technical Report*, Vol.2015-CH-108, No.5, pp.1-6 (2015) (in Japanese).
- [9] Miura, T., Kaiga, T., Shibata, T., Tajima, K. and Tamamoto, H.: Low-dimensional Feature Vector Extraction from Motion Capture Data by Phase Plane Analysis, *Journal of Information Processing*, Vol.25, pp.884-887 (2017).
- [10] Bartlett, R.: *Introduction to Sports Biomechanics*, 2nd ed., Routledge (2007).
- [11] Rubner, Y., Tomasi, C. and Guibas, L.J.: The Earth Mover's Distance as a Metric for Image Retrieval, *International Journal of Computer Vision*, Vol.40, No.2, pp. 99-121 (2000).
- [12] For example, Johnson, R. A. and Wichern, D. W.: *Applied Multivariate Statistical Analysis*, 6th ed., Pearson Education Inc. (2007).